



A Possible γ -Ray Pulsation from PSR J1740–5340B in the Globular Cluster NGC 6397

Jiao Zheng, Pengfei Zhang, and Li Zhang

Department of Astronomy, School of Physics and Astronomy, Key Laboratory of Astroparticle Physics of Yunnan Province, Yunnan University, Kunming 650091, China; zhangpengfei@ynu.edu.cn, lizhang@ynu.edu.cn

Received 2023 October 20; revised 2023 November 16; accepted 2023 November 30; published 2024 January 17

Abstract

Recently, a new radio millisecond pulsar (MSP) J1740–5340B, hosted in the globular cluster (GC) NGC 6397, was reported with a 5.78 ms spin period in an eclipsing binary system with a 1.97 days orbital period. Based on a modified radio ephemeris updated by tool tempo2, we analyze the ~ 15 yr γ -ray data obtained from the Large Area Telescope on board the Fermi Gamma-ray Space Telescope and detect PSR J1740–5340B's γ -ray pulsation at a confidence level of $\sim 4\sigma$ with a weighted H -test value of ~ 26 . By performing a phase-resolved analysis, the γ -ray luminosity in on-pulse interval of PSR J1740–5340B is $L_\gamma \sim 3.8 \times 10^{33}$ erg s $^{-1}$ using NGC 6397's distance of 2.48 kpc. And γ -rays from the on-pulse part of PSR J1740–5340B contribute $\sim 90\%$ of the total observed γ -ray emissions from NGC 6397. No significant γ -ray pulsation of another MSP J1740–5340A in the GC is detected. Considering that the previous four cases of MSPs in GCs, more data in γ -ray, X-ray, and radio are encouraged to finally confirm the γ -ray emissions from MSP J1740–5340B, especially starving for a precise ephemeris.

Key words: gamma-rays: galaxies – (stars:) pulsars: individual (PSR J1740-5340B) – (Galaxy:) globular clusters: individual (NGC 6397)

1. Introduction

Globular clusters (GCs) are ancient celestial systems with typical age of over 10^{10} yr, they hold together by stellar mutual gravity orbiting the Milky Way (e.g., Harris 1996) as satellites. The extremely high stellar density ($\sim 10^{3-6}$ stars pc $^{-3}$) in GCs' cores provides conditions for stellar interactions to form low mass X-ray binaries (LMXBs). The formation rates in GCs are more than two orders of magnitude higher than those in other regions of the Galaxy (Clark 1975; Katz 1975). The millisecond pulsars (MSPs) are thought to be “recycled” pulsars by the accretion of mass and angular momentum from a companion star in the mass-transfer binaries, then they are spun up to short spin periods of several milliseconds. Therefore, LMXBs are generally believed to be the progenitors of MSPs. It is generally believed that GCs are among the most prolific environments for the formation of MSPs (Alpar et al. 1982; Bhattacharya & van den Heuvel 1991). Since the first MSP was detected in GC (M28, aka NGC 6626) by the Lovell 76 m radio telescope (Lyne et al. 1987), about 272 pulsars have been observed in 38 GCs¹ within 20 kpc of the center of the Galaxy, more than 90% of them are MSPs, and 50% MSPs are located in binary systems. While, usually, radio MSPs are mostly associated with γ -ray sources.

Thanks to the Large Area Telescope (LAT) on board Fermi Gamma-ray Space Telescope (Fermi-LAT; Atwood et al. 2009),

γ -ray emissions from GCs were first detected in GC 47 Tucanae (Abdo et al. 2009). Up to now, approximately 40 GCs' γ -rays have been detected in the fourth Fermi-LAT source catalog for Data Release 3 (4FGL-DR3; Abdollahi et al. 2022) and Abdo et al. (2010a), Kong et al. (2010), Tam et al. (2011), Eger & Domainko (2012), Zhou et al. (2015), Tam et al. (2016), Zhang et al. (2016), Lloyd et al. (2018), MAGIC Collaboration et al. (2019), Ndiyavala et al. (2019), MAGIC Collaboration et al. (2019), Abdollahi et al. (2020); Ballet et al. (2020); Song et al. (2021); Yuan et al. (2022a, 2022b); Abdollahi et al. (2022); Wu et al. (2022). In GC, the first γ -ray pulsation from an individual pulsar, PSR J1823–3021A, was also reported in NGC 6624 (Freire et al. 2011) with a 5.44 ms spin period (P) and a larger spin-down rate of $\dot{P} = 3.38 \times 10^{-18}$ s s $^{-1}$, its spin-down luminosity is $\dot{E} = 8.3 \times 10^{35}$ erg s $^{-1}$. Followed by an MSP in NGC 6626 (M28), Wu et al. (2013) and Johnson et al. (2013) independently reported a discovery of γ -ray pulsation with a frequency consistent with MSP B1821–24, its spin period and spin-down rate are $P = 3.05$ ms and $\dot{P} = 1.61 \times 10^{-18}$ s s $^{-1}$, respectively, and the spin-down luminosity is $\dot{E} = 2.2 \times 10^{36}$ erg s $^{-1}$. Then in NGC 6652, Zhang et al. (2022b) reported a detection of γ -ray pulsation from PSR J1835–3259B. For this MSP, its spin period and the spin-down rate are $P = 1.83$ ms and $\dot{P} = 1.61 \times 10^{-18}$ s s $^{-1}$, respectively, reported in Gautam et al. (2022), its \dot{E} is $\sim 4.3 \times 10^{35}$ erg s $^{-1}$. Recently, Zhang et al. (2023) reported the fourth γ -ray pulsation of PSR J1717+4308A in NGC 6341 with the radio rotational ephemeris reported in Pan

¹ <http://www.naic.edu/~pfreire/GCpsr.html>

et al. (2020). Above mentioned reports seem to indicate that γ -ray emissions from GCs primarily arise from an individual MSPs hosted within them.

NGC 6397 is located at a 2.48 kpc distance (Baumgardt & Vasiliev 2021) from the Sun in the southern constellation of Ara, putting it one of the two closest GCs. Its age was estimated to be 12.6 billion years old in Correnti et al. (2018). In this GC, the first MSP J1740–5340A (at R.A. = $17^{\text{h}}40^{\text{m}}44^{\text{s}}.589$ and decl. = $-53^{\circ}40'40''$ 90) with a 3.65 ms spin period was reported by D’Amico et al. (2001), Ferraro et al. (2001), Grindlay et al. (2001), Bogdanov et al. (2010) in an eclipsing binary system with a 1.35 days orbital period. Recently, Zhang et al. (2022a) reported another new discovery of a radio MSP, PSR J1740–5340B, with 5.78 ms spin period in an eclipsing binary system with a 1.97 days orbital period (at R.A. = $17^{\text{h}}40^{\text{m}}42^{\text{s}}.626$ and decl. = $-53^{\circ}40'27''$ 91) by the Parkes radio telescope (also named as Murriyang) with the observing frequency band from 704 to 4032 MHz in Australia and the MeerKAT radio telescope with frequency band of 856–1712 MHz in South Africa. The second MSP’s spin-down period derivative (\dot{P}) is $-5.93 \times 10^{-21} \text{ s s}^{-1}$. Here, we updated the MSP’s radio ephemeris provided in Zhang et al. (2022a) with the ~ 15 yr Fermi-LAT data by employing tool tempo2. Then we carried out a detailed data analysis for the events around NGC 6397 collected by the Fermi-LAT and detected a γ -ray pulsation from MSP J1740–5340B at a post-trial significance of $\sim 4\sigma$, which corresponds to a weighted H -test value of ~ 26 . By performing a phase-resolved analysis, the γ -ray emissions from the on-pulse interval contribute $\sim 90\%$ of the total observed γ -rays from NGC 6397. Comparing to the previous four cases, this is the only one γ -ray MSP in GC with a spin-up period. The paper is organized as follows. We describe the data analysis for the Fermi-LAT and report the main results in Section 2 followed by timing analysis in Section 3. Summaries and discussions of our γ -ray results are shown in Section 4.

2. Fermi-LAT Data Analysis and Results

NGC 6397’s γ -ray emissions have been first detected by Zhang et al. (2016). In the fourth Fermi-LAT catalog Data Release 3 (4FGL-DR3), a γ -ray source named 4FGL J1741.1–5341 associated with NGC 6397 was cataloged in Abdollahi et al. (2020), Ballet et al. (2020), and Abdollahi et al. (2022), it was also presented in the Fermi-LAT eight year sources named as FL8Y J1741.2-5342.

2.1. Data Preparation and Source Model

The LAT is a pair conversion telescope on board the Fermi satellite sensitive to γ -rays with energy range from ~ 20 MeV to >500 GeV. In our data analysis, we selected the LAT events in the time range between 2008 August 4 and 2023 May 15 (MJD 54,683 to MJD 60,079) with energies between 0.1 and

Table 1
Best-fit Results from Likelihood Analysis

Models	Parameter Values			
LP	α	β	E_b (GeV)	TS
	2.6(2) ^a	0.3(1) ^a	1.2 ^a	...
	2.5(2)	0.4(1)	1.2(2)	79.8
PLEC	Γ	b	E_c (GeV)	TS
	2.0(2)	2/3	3.0(5)	81.8
	P_{on}	2/3	1.3(5)	76.9
P_{off}	2.0	2/3	3.0	8.9

Note.

^a Parameter values provided in 4FGL-DR3 for the LP model, while the error of E_b not given in 4FGL-DR3. The numbers in parentheses is their errors, the value of b for the PLEC model was fixed at 2/3 in all the data analysis.

500.0 GeV centered on 4FGL J1741.1–5341 with a coordinate at R.A. = $17^{\text{h}}41^{\text{m}}09^{\text{s}}.790$ and decl. = $-53^{\circ}41'02''$ 419 (Abdollahi et al. 2022). Around the target, the latest Pass 8 (with evclass = 128 and evtype = 3) SOURCE class events within a $20^{\circ} \times 20^{\circ}$ region of interest (RoI) were selected for the whole data analysis. The events with zenith angle $>90^{\circ}$ were removed to minimize the contamination of the background γ -rays from the Earth’s limb. We used a filter expression of “(DATA_QUAL>0) && (LAT_CONFIG==1)” to obtain the high quality data in good time intervals. The instrumental response function of “P8R3_SOURCE_V3” and the FermiTools with version of 2.2.0 were used in the our data analysis.²

To obtain the best-fit parameters of NGC 6397, a model file was created based on the 4FGL-DR3 catalog by a script make4FGLxml.py,³ which including of γ -ray sources within a 25° radius as well as two diffuse emission background components: Galactic and extragalactic isotropic diffuse emissions. We freed the flux normalizations and spectral shape parameters for the sources within 5° from 4FGL J1741.1–5341, the normalizations for the sources within 5° – 10° , and the normalizations of two diffuse backgrounds. While other γ -ray sources’ parameters were fixed at their values provided in the 4FGL-DR3.

Then a binned maximum likelihood analysis was performed between the whole data and the model file to derive the best-fit parameters. A best-fit model file was built for all the γ -ray sources in the file. In 4FGL-DR3, 4FGL J1741.1–5341 has a log-parabola spectral shape (LP) with a formula of $dN/dE = N_0(E/E_b)^{-\alpha-\beta \log(E/E_b)}$. An average photon flux was obtained at a value of $(3.7 \pm 0.8) \times 10^{-9}$ photons $\text{cm}^{-2} \text{s}^{-1}$ in the 0.1–500.0 GeV energies. The best-fit spectral parameters are listed in Table 1. Their values are in good agreement with that

² <https://github.com/fermi-lat/Fermitools-conda/wiki/Installation-Instructions>

³ <https://fermi.gsfc.nasa.gov/ssc/data/analysis/user/>

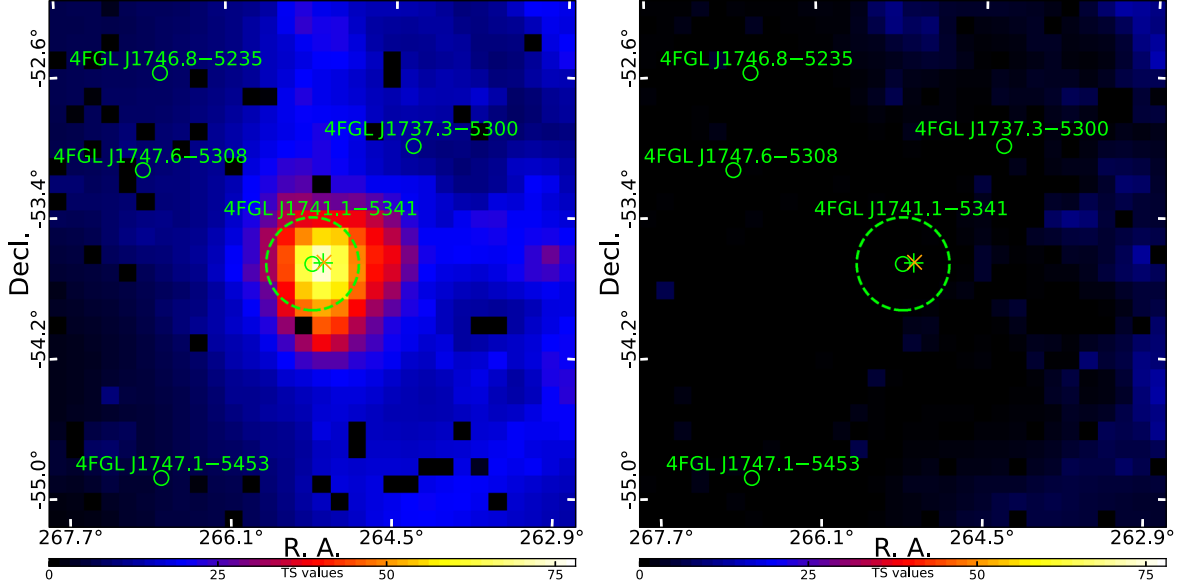


Figure 1. Two TS maps with $3^\circ \times 3^\circ$ region centered at the position of 4FGL J1741.1–5341 in 0.1–500.0 GeV. Left panel: the TS map was created by removing the target in the best-fit model to show the γ -ray emissions from NGC 6397. Right panel: residual TS map was created based on the best-fit model (NGC 6397 had a PLEC spectral shape). The γ -ray sources reported in the 4FGL-DR3 are shown with the green circles. The green dashed circle stands for NGC 6397’s tidal radius centered at 4FGL J1741.1–5341. MSPs J1740–5340A and J1740–5340B are marked with a green plus and an orange cross, respectively. The two TS maps share the same color-bar and have pixels $0^\circ.1$ on one side.

reported in 4FGL-DR3. Considering that γ -rays of GCs likely arising from those MSPs hosted within themselves, a spectral model of a power law with an exponential cutoff (PLEC), $dN/dE = N_0(E/E_0)^{-\Gamma} \exp[-(E/E_c)^b]$, was used to model the γ -rays from NGC 6397. The PLEC is a typical model for describing the pulsars’ spectral energy distribution (SED) in energies of 0.1–500.0 GeV. For PLEC model, the best-fit parameter values are listed in Table 1. The TS value of PLEC model was 81.8, the average photon flux was $(6.6 \pm 0.9) \times 10^{-9}$ photons $\text{cm}^{-2} \text{s}^{-1}$ in 0.1–500.0 GeV, and the integrated energy flux was $(3.5 \pm 0.4) \times 10^{-12}$ erg $\text{cm}^{-2} \text{s}^{-1}$. Comparing the best-fit results of two spectral models of LP and PLEC, the TS value from PLEC model is slightly larger than that from LP model. The best-fit parameters with PLEC model for target were saved as a best-fit model, and the following analysis was carried out based on them. Considering the distance of NGC 6397 at 2.48 ± 0.02 kpc (Baumgardt & Vasiliev 2021), its γ -ray luminosity is $(2.5 \pm 0.3) \times 10^{33}$ erg s^{-1} under the assumption of isotropic emission.

2.1.1. TS Maps Extraction

To reveal the γ -ray emissions from NGC 6397, a TS map with $3^\circ \times 3^\circ$ region centered at the coordinate of 4FGL J1741.1–5341 in 0.1–500.0 GeV was created by employing the Tool *gttsmap* and basing on the best-fit model and removing 4FGL J1741.1–5341 in the model, and it is shown in left panel of Figure 1. In order to exclude the contamination from the new

possible nearby γ -ray sources (not included in 4FGL-DR3), a residual TS map was created based on the above best-fit model, which has the same spatial size as the TS map. We show the residual TS map in right panel of Figure 1. In the figure, the maximum of TS values at all the pixels is 13.4, far less than 25 (which is corresponding to a detection significance of $\sim 4\sigma$). That is, no new γ -ray source appears around the target. From the residual map, we believe that the whole γ -ray events around the target are well described by the γ -ray sources in the best-fit model file. After comparing with the two maps, we think that a point source with a PLEC spectral model can describe γ -ray emissions from NGC 6397 in 0.1–500.0 GeV very well. We also show the two MSPs, J1740–5340A and J1740–5340B, with a green plus and an orange cross in Figure 1, respectively.

2.1.2. Spectrum Extraction

We performed a spectral analysis based on the best-fit model. In this step, for the model file, we only freed the normalizations of the sources within 10° and the two background components, and other parameters of spectral shapes were fixed at their best-fit values for all the sources in the model file. We divided the 0.1–500.0 GeV energy range into 12 equal logarithmically spaced energy bins, and obtained flux of NGC 6397 for each energy bin by employing the binned likelihood analysis. The flux data points (i.e., SED) were derived and shown in Figure 2, in which the data points with

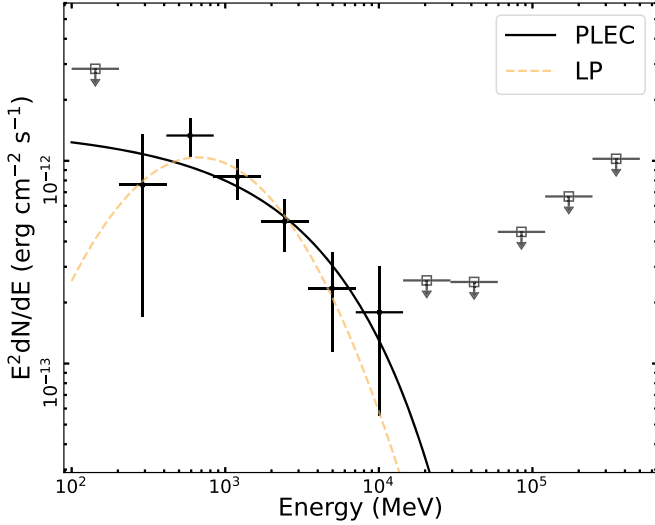


Figure 2. γ -ray SED of NGC 6397 in 0.1–500.0 GeV. The data points were derived from the maximum likelihood analysis in the individual energy band based on the PLEC model of the target, in which the flux data points with TS values ≥ 5 were kept, otherwise they are shown with their 95% flux upper limits. The black solid and orange dashed lines stand for the best-fit PLEC and LP models derived from the whole data analysis.

TS ≥ 5 were kept, other ones were shown with their 95% flux upper limits. From Figure 2, we can see that γ -ray SED of NGC 6397 is well described by a PLEC model.

3. Timing Analysis

3.1. γ -Ray Pulse Profile

Due to the large point-spread function of the Fermi-LAT, these two MSPs, J1740-5340A and J1740-5340B, in NGC 6397 cannot be identified as two independent γ -ray sources. In our analysis, if we folded the γ -rays from the GC based on the ephemeris of one pulsar, and the γ -rays from another will serve as the background, evenly distributed in the phase-resolved light curve. First, based on the ephemeris provided by Zhang et al. (2022a), we carried out a timing analysis of the 0.1–500.0 GeV events around NGC 6397 within an aperture radius of $3^{\circ}16'$, this selection criterion of angle $\theta < \max(6.68 - 1.76 \log_{10}(E_{\text{MeV}}), 1.3)^{\circ}$ was adopted as them shown in Abdo et al. (2010b). While no significant pulse profile was detected over the ~ 15 yr Fermi-LAT observations. Then we used the γ -ray data to update the radio ephemeris by determining the pulse times of arrival and cross-correlated the pulse profiles by employing the tool tempo2⁴ (Hobbs et al. 2006). A similar process has been executed in Xing & Wang (2015) and Xing et al. (2022). In our analysis, the timing parameters, the frequency derivatives from f_0 to f_2 , were fixed at their known values that provided in Zhang et al. (2022a),

⁴ <https://sourceforge.net/projects/tempo2/>

only the higher order frequency derivatives (f_3 – f_6) were fitted, which provided in a supplementary material (named “ngc6397b.tar”). Then we assigned pulse phases for the events by employing the tool tempo2 with the Fermi plug-in (Ray et al. 2011). Their probabilities that originating from NGC 6397 were calculated with the Fermi tool gtsrcprob as their weights for the γ -ray events, the largest probability is 70.3%.

In consideration of the fainter γ -ray flux of NGC 6397 comparing with other γ -ray pulsars in 4FGL-DR3, the folded weighted γ -ray pulse profile was binned into ten phase intervals. We show the γ -ray pulse profile and a two-dimensional phaseogram in panels (A) and (B) of Figure 3, respectively. In the folded pulse profile, the count uncertainties for the phase bins were calculated following the method provided by Abdo et al. (2013). We also estimated the background counts contribution from the two diffuse sources and the neighboring γ -ray sources around 4FGL J1741.1–5341 in the 4FGL-DR3. Its value is ~ 119.6 shown with a horizontal red dashed-dotted line in Figure 3, which is well in agreement with that lowest phase bin (119.4 ± 2.3) of the pulse profile at the fourth bin.

An H -test statistic was applied to the events considering that their pulse phases and the corresponding probabilities by the method provided by de Jager & Büsching (2010) and Kerr (2011). The curve of cumulative H -test values spanning the Fermi-LAT observations is shown in Figure 3(C). An H -test value of 25.8 is obtained, which corresponds to a p -value of 3.3×10^{-5} ($\sim 4.2\sigma$), it was given by $p\text{-value} = e^{-0.4 \times H}$. Our calculation is in agreement with those reported in Kerr (2011), Abdo et al. (2013), Smith et al. (2019).

The radio pulse profile of PSR J1740–5340B is shown in panel (D) of Figure 3, which is drawn approximately from that reported in Zhang et al. (2022a).

We also carried out the same timing analysis for another MSP, PSR J1740–5340A, with the radio ephemeris reported by Ferraro et al. (2001), Grindlay et al. (2001), Bogdanov et al. (2010). While no significant γ -ray pulsation with a frequency consistent with the MSP is detected. Considering this trial factor, the trial number (N) is two. The false-alarm probability (FAP) was estimated by $\text{FAP} = 1 - (1 - p)^N \sim 6.6 \times 10^{-5}$, which is corresponding to $\sim 4.0\sigma$.

3.2. Phase-resolved Analysis

Based on the γ -ray pulse profile (Figure 3(A)), we defined the on-pulse phase interval (P_{on}) in phase of 0.7–1.3, and the off-pulse (P_{off}) in 0.3–0.7 phase, and they are shown in the Figure 3(A) with pink and blue shaded regions, respectively. Then we performed likelihood analysis for the events from on- and off-pulse intervals using the PLEC model to describe the corresponding γ -ray emissions from NGC 6397, and summarized the best-fit parameters in Table 1. For the on-pulse data, PSR J1740–5340B’s γ -ray luminosity is $L_{\gamma} = (3.8 \pm 0.9) \times 10^{33} \text{ erg s}^{-1}$. For off-pulse, its

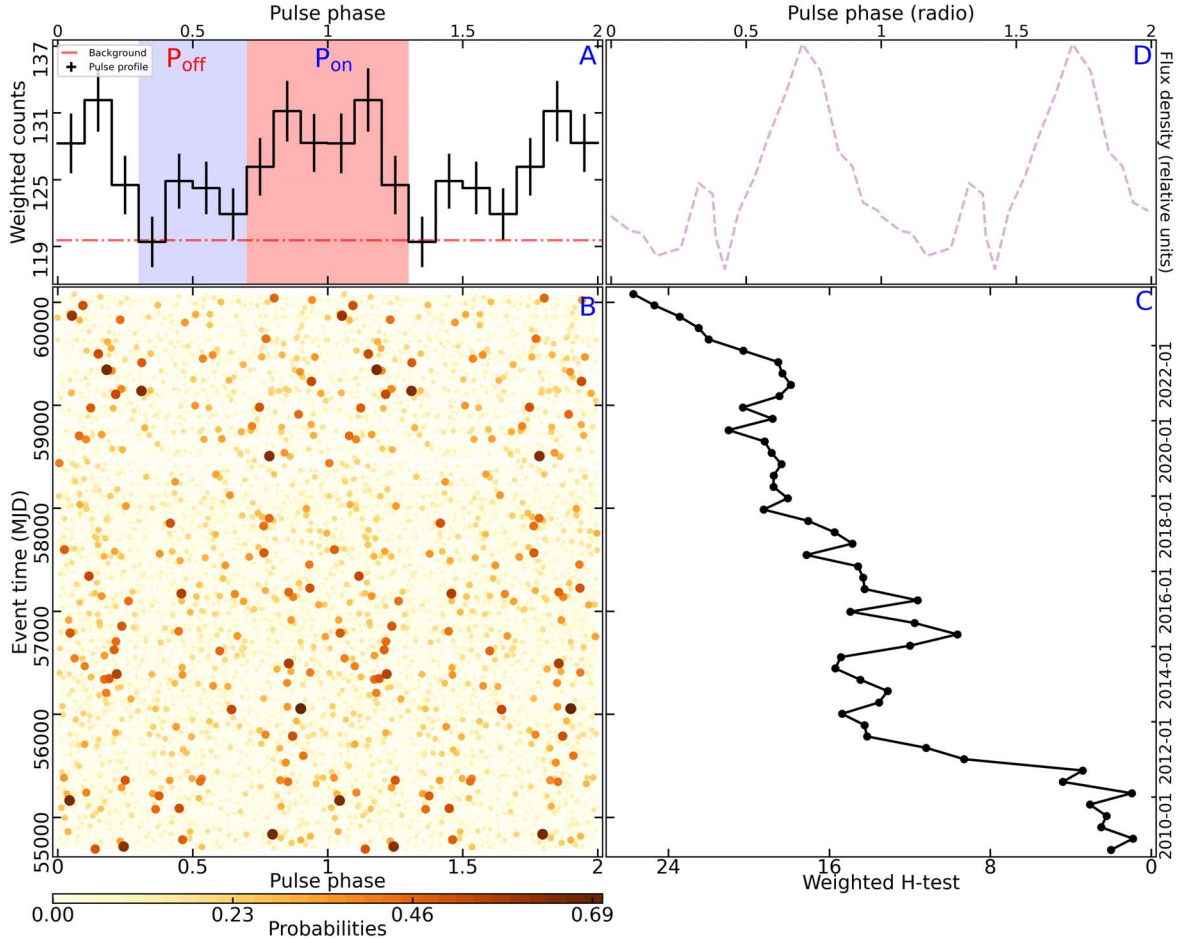


Figure 3. Weighted γ -ray timing analysis results of PSR J1740–5340B in 0.1–500.0 GeV. Panel (A): the MSP’s weighted γ -ray pulse profile (ten phase intervals), which is shown over two rotations for clarity. The on- and off-pulse phase intervals are colored with pink and blue shaded regions, respectively. The horizontal red dashed–dotted line stands for the background counts. Panel (B): two-dimensional phaseogram, the points stand for γ -rays originating from NGC 6397 with coded colors indicating the probabilities. Panel (C): the weighted H -test values over the whole observations of Fermi-LAT. Panel (D): the MSP’s radio pulse profile in the frequency band of ~ 0.7 –4.0 GHz approximately derived from Zhang et al. (2022a).

γ -ray luminosity is $L_\gamma = (0.4 \pm 0.3) \times 10^{33} \text{ erg s}^{-1}$. Their TS values were ~ 76.9 and 8.9 , respectively. In the likelihood analysis of the off-pulse data, we fixed the parameters of spectral shape at the values from the best-fit model because the target is not very significant in this phase interval. Based on the likelihood analysis results of on- and off-pulse intervals, their TS maps (with the same region size as shown in Figure 1) were obtained by removing the target in the model files and are shown in Figure 4. Therefore, the γ -ray emissions from the on-pulse interval contribute $\sim 90\%$ of the total observed γ -rays from NGC 6397.

4. Conclusion and Discussion

In 4FGL-DR3, approximately 40 GCs have been detected with γ -ray emissions. In them, their γ -ray emissions are typically believed to originate from the collective contribution of a large number of pulsars harbored within them. In NGC

6397, two MSPs, J1740-5340A and J1740-5340B, were detected in radio telescopes (D’Amico et al. 2001; Zhang et al. 2022a). Several scenarios have been proposed to explain the radiation mechanism of γ -rays from GCs. According to the pulsar magnetosphere model, pulsars are believed to emit γ -rays in the several GeV through curvature radiation (Zhang & Cheng 2003). Additionally, as suggested in Du et al. (2012), it is claimed that GeV γ -rays can be produced through inverse Compton scattering processes involving surrounding soft photons and energetic electrons/positrons. Motivated by the discovery of the MSP J1740–5340B (Zhang et al. 2022a), we carried out the data analysis for the γ -ray emissions from NGC 6397 by the Fermi-LAT observations spanning from 2008 August 4 to 2023 May 15. Based on the updated radio ephemeris, we performed a timing analysis and detected of γ -ray pulsation with a frequency consistent with the newly

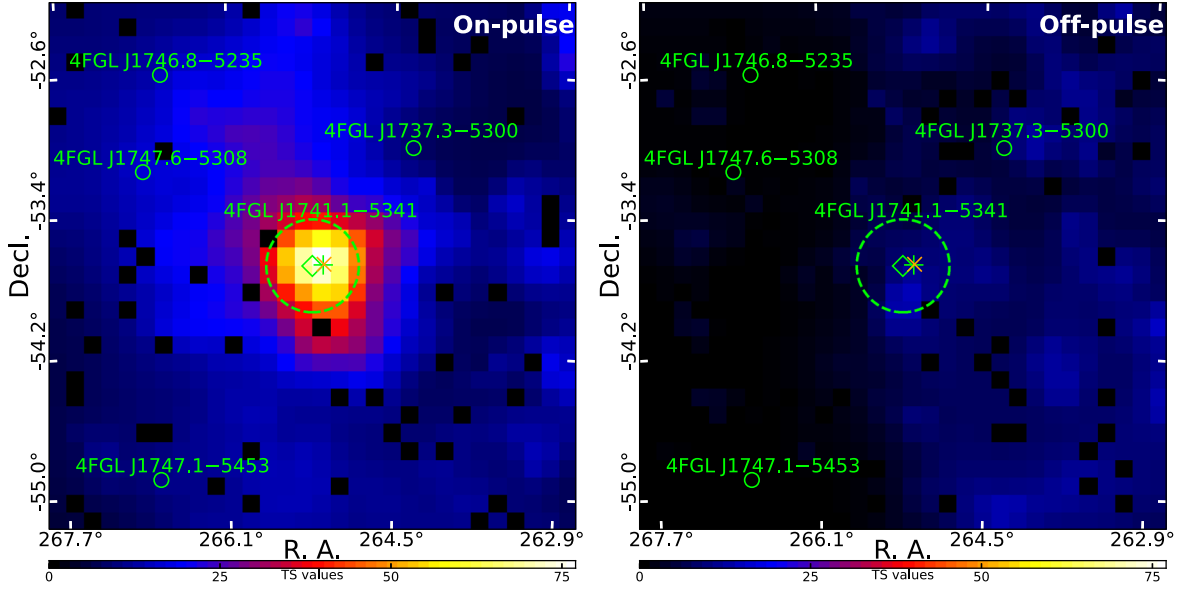


Figure 4. On- and off-pulse TS maps of PSR J1740–5340B, which were created with Fermi-LAT data in the on- and off-pulse phase intervals. Others are same as in the Figure 1.

discovered MSP at a $\sim 4\sigma$ confidence level. This positions it as the fifth γ -ray MSP discovered within the GC and notably, the first one exhibiting a spin-up period. The TS maps and SEDs of NGC 6397 were obtained based on PLEC spectral model in 0.1–500.0 GeV and are shown in Figures 1 and 2, respectively. From the residual TS map (shown in the right panel of Figure 1), it can be concluded that a γ -ray point-like source described by a PLEC model effectively characterizes the γ -ray emissions of NGC 6397.

By the timing analysis, the background counts contribution from the two diffuse sources and neighboring γ -ray sources in the model file were estimated, and its result is shown in Figure 3(A) with a red dashed–dotted line. The value is well in agreement with that lowest count bin of the γ -ray pulse profile. This implies that the γ -rays from PSR J1740–5340B account for the most of the observed γ -ray emissions (90%) from the GC NGC 6397. Other 10% γ -ray emissions may come from the off-pulse of PSR J1740–5340B or/and the first pulsar J1740–5340A. This is also consistent with the off-pulse TS map in the phase-resolved analysis (shown in the right panel of Figure 4). Similar results have been reported for PSR J1835–3259B in NGC 6652 and PSR J1717+4308A in NGC 6341 by Zhang et al. (2022b, 2023), in which the pulsed γ -ray component also contributes the most of total observed γ -rays from the GCs.

In the phase-resolved analysis, the TS values of on- and off-pulse intervals are ~ 76.9 and 8.9, respectively. This result may strengthen our discovery of the γ -ray pulsation from PSR J1740–5340B. The on-pulse (off-pulse) luminosity is $L_\gamma \sim 3.8 \times 10^{33} \text{ erg s}^{-1}$ ($\sim 0.4 \times 10^{33} \text{ erg s}^{-1}$). Based on the

assumption that MSPs share the same characteristics and emit similar amount of γ -rays in the GCs, we can use the observed γ -ray luminosity to estimate the number of MSPs expected hosted within each GC. Using the off-pulse luminosity, we estimated the number of other MSPs (N_{MSPs}) hosted within NGC 6397 is ~ 0.2 by a formula of $N_{\text{MSPs}} = L_\gamma / \langle \dot{E} \rangle \langle \eta_\gamma \rangle$, where $\langle \dot{E} \rangle$ is the MSPs’ average spin-down power and $\langle \eta_\gamma \rangle$ is the estimated average spin-down to γ -ray luminosity conversion efficiency. The value of $\langle \dot{E} \rangle$, $3.0 \times 10^{34} \text{ erg s}^{-1}$, was estimated by the averaged from Galactic field MSPs in the ATNF pulsar catalog.⁵ While the value of $\langle \eta_\gamma \rangle$ of 0.08 was derived from observations of the three nearest known MSPs as it adopted in Abdo et al. (2009). We know that the intrinsic spin-down of MSPs is masked by the cluster’s acceleration, and the measurement of \dot{P} is not accurate, making it difficult to estimate \dot{E} for MSPs in GCs. Hence our estimation is rather rough.

No significant difference was found between this γ -ray PSR J1740–5340B and the previous ones detected in GCs reported in Freire et al. (2011), Johnson et al. (2013), Wu et al. (2013), Zhang et al. (2022b, 2023) in terms of the γ -ray SEDs and the numbers of known MSPs, in summary those four MSPs are younger MSPs. Three of them have higher spin-down luminosities of $(0.4 - 2.2) \times 10^{36} \text{ erg s}^{-1}$ (Freire et al. 2011; Johnson et al. 2013; Wu et al. 2013; Zhang et al. 2022b), they are among the more brighter MSPs known than the typical ones. While PSR J1717+4308A has more lower luminosity in γ -rays. Nevertheless, PSR J1740–5340B hosted in the nearest

⁵ <https://www.atnf.csiro.au/research/pulsar/psrcat/>

NGC 6397 locates at a 2.48 kpc distance (one of the two nearest GCs), this may be the reason that its γ -ray pulsation is detected by Fermi-LAT. We also show the schematic radio pulse profile from Zhang et al. (2022a) in Figure 3(D), it is just to facilitate the comparison of γ -ray and radio pulse profiles and not for alignment of them. We know that the technical of alignment of the radio and γ -ray pulse profiles is actually quite difficult. Moreover, there are not enough information in the ephemeris provided by Zhang et al. (2022a) for establishing the alignment, and the ephemeris used in this work is modified by Fermi-LAT data. Hence we do not delve the topics of alignment between γ -ray and radio pulse profiles.

To confirm the γ -ray pulsation of PSR J1740–5340B, more data by γ -ray, X-ray, and radio telescopes are encouraged, especially starving for a precise ephemeris. The future γ -ray telescopes, e.g., Very Large Area Gamma-ray Space Telescope (VLASt, Fan et al. 2022), may provide additional insights into this pulsar and the related studies of γ -rays from GCs.

Acknowledgments

We thank an anonymous referee for the comments that helped improve this work. This work is supported in part by the National Natural Science Foundation of China Nos. 12163006 and 12233006, the Basic Research Program of Yunnan Province No. 202201AT070137, and the joint foundation of Department of Science and Technology of Yunnan Province and Yunnan University No. 202201BF070001-020. P. F. Zhang acknowledges the support by the Xingdian Talent Support Plan - Youth Project.

Data Availability

The data underlying this work can be made available in Fermi Science Support Center.⁶

References

- Abdo, A. A., Ackermann, M., Ajello, M., et al. 2009, *Sci*, **325**, 845
 Abdo, A. A., Ackermann, M., Ajello, M., et al. 2010a, *A&A*, **524**, A75
 Abdo, A. A., Ackermann, M., Ajello, M., et al. 2010b, *ApJ*, **708**, 1254
 Abdo, A. A., Ajello, M., Allafort, A., et al. 2013, *ApJS*, **208**, 17
 Abdollahi, S., Acero, F., Ackermann, M., et al. 2020, *ApJS*, **247**, 33
 Abdollahi, S., Acero, F., Baldini, L., et al. 2022, *ApJS*, **260**, 53
 Alpar, M. A., Cheng, A. F., Ruderman, M. A., & Shaham, J. 1982, *Natur*, **300**, 728
 Atwood, W. B., Abdo, A. A., Ackermann, M., et al. 2009, *ApJ*, **697**, 1071
 Ballet, J., Burnett, T. H., Digel, S. W., & Lott, B. 2020, arXiv:2005.11208
 Baumgardt, H., & Vasiliev, E. 2021, *MNRAS*, **505**, 5957
 Bhattacharya, D., & van den Heuvel, E. P. J. 1991, *PhR*, **203**, 1
 Bogdanov, S., van den Berg, M., Heinke, C. O., et al. 2010, *ApJ*, **709**, 241
 Clark, G. W. 1975, *ApJL*, **199**, L143
 Correnti, M., Gennaro, M., Kalirai, J. S., Cohen, R. E., & Brown, T. M. 2018, *ApJ*, **864**, 147
 D’Amico, N., Possenti, A., Manchester, R. N., et al. 2001, *ApJL*, **561**, L89
 de Jager, O. C., & Büsching, I. 2010, *A&A*, **517**, L9
 Du, Y. J., Qiao, G. J., & Wang, W. 2012, *ApJ*, **748**, 84
 Eger, P., & Domainko, W. 2012, *A&A*, **540**, A17
 Fan, Y. Z., Chang, J., Guo, J. H., et al. 2022, *AcASn*, **63**, 27
 Ferraro, F. R., Possenti, A., D’Amico, N., & Sabbi, E. 2001, *ApJL*, **561**, L93
 Freire, P. C. C., Abdo, A. A., Ajello, M., et al. 2011, *Sci*, **334**, 1107
 Gautam, T., Ridolfi, A., Freire, P. C. C., et al. 2022, *A&A*, **664**, A54
 Grindlay, J. E., Heinke, C. O., Edmonds, P. D., Murray, S. S., & Cool, A. M. 2001, *ApJL*, **563**, L53
 Harris, W. E. 1996, *AJ*, **112**, 1487
 Hobbs, G., Edwards, R., & Manchester, R. 2006, *ChJAS*, **6**, 189
 Johnson, T. J., Guillemot, L., Kerr, M., et al. 2013, *ApJ*, **778**, 106
 Katz, J. I. 1975, *Natur*, **253**, 698
 Kerr, M. 2011, *ApJ*, **732**, 38
 Kong, A. K. H., Hui, C. Y., & Cheng, K. S. 2010, *ApJL*, **712**, L36
 Lloyd, S. J., Chadwick, P. M., & Brown, A. M. 2018, *MNRAS*, **480**, 4782
 Lyne, A. G., Brinklow, A., Middleditch, J., Kulkarni, S. R., & Backer, D. C. 1987, *Natur*, **328**, 399
 MAGIC Collaboration, Acciari, V. A., Ansoldi, S., et al. 2019, *MNRAS*, **484**, 2876
 Ndiyavala, H., Venter, C., Johnson, T. J., et al. 2019, *ApJ*, **880**, 53
 Pan, Z., Ransom, S. M., Lorimer, D. R., et al. 2020, *ApJL*, **892**, L6
 Ray, P. S., Kerr, M., Parent, D., et al. 2011, *ApJS*, **194**, 17
 Smith, D. A., Bruel, P., Cognard, I., et al. 2019, *ApJ*, **871**, 78
 Song, D., Macias, O., Horiuchi, S., Crocker, R. M., & Nataf, D. M. 2021, *MNRAS*, **507**, 5161
 Tam, P.-H. T., Hui, C. Y., & Kong, A. K. H. 2016, *JASS*, **33**, 1
 Tam, P. H. T., Kong, A. K. H., Hui, C. Y., et al. 2011, *ApJ*, **729**, 90
 Wu, J. H. K., Hui, C. Y., Wu, E. M. H., et al. 2013, *ApJL*, **765**, L47
 Wu, W., Wang, Z., Xing, Y., & Zhang, P. 2022, *ApJ*, **927**, 117
 Xing, Y., & Wang, Z. 2015, *ApJL*, **804**, L33
 Xing, Y., Zheng, D., Wang, Z., et al. 2022, *ApJ*, **930**, 164
 Yuan, M., Ren, C., Zhang, P., Jiang, Z., & Zhang, L. 2022a, *RAA*, **22**, 115013
 Yuan, M., Zheng, J., Zhang, P., & Zhang, L. 2022b, *RAA*, **22**, 055019
 Zhang, L., & Cheng, K. S. 2003, *A&A*, **398**, 639
 Zhang, L., Ridolfi, A., Blumer, H., et al. 2022a, *ApJL*, **934**, L21
 Zhang, P., Xing, Y., Wang, Z., et al. 2023, *ApJ*, **945**, 70
 Zhang, P., Xing, Y., & Wang, Z. 2022b, *ApJL*, **935**, L36
 Zhang, P. F., Xin, Y. L., Fu, L., et al. 2016, *MNRAS*, **459**, 99
 Zhou, J. N., Zhang, P. F., Huang, X. Y., et al. 2015, *MNRAS*, **448**, 3215

⁶ <https://heasarc.gsfc.nasa.gov/FTP/fermi/data/lat/weekly/photon/>